Mediated Interaction between Ions in Quantum Degenerate Gases

Shanshan Ding[◎],[1] Michael Drewsen,[1] Jan J. Arlt[◎],[1] and G. M. Bruun[◎][1,2,*]

[1]*Center for Complex Quantum Systems, Department of Physics and Astronomy, Aarhus University,*
Ny Munkegade, DK-8000 Aarhus C, Denmark
[2]*Shenzhen Institute for Quantum Science and Engineering and Department of Physics,*
Southern University of Science and Technology, Shenzhen 518055, China

We explore the interaction between two trapped ions mediated by a surrounding quantum degenerate Bose or Fermi gas. Using perturbation theory valid for weak atom-ion interaction, we show analytically that the interaction mediated by a Bose gas has a power-law behavior for large distances whereas it has a Yukawa form for intermediate distances. For a Fermi gas, the mediated interaction is given by a power law for large density and by a Ruderman-Kittel-Kasuya-Yosida form for low density. For strong atom-ion interaction, we use a diagrammatic theory to demonstrate that the mediated interaction can be a significant addition to the bare Coulomb interaction between the ions, when an atom-ion bound state is close to threshold. Finally, we show that the induced interaction leads to substantial and observable shifts in the ion phonon frequencies.

Introduction.—Mediated interactions play a crucial role for our understanding of nature. They are central to Landau's widely used quasiparticle theory [1], and all interactions are mediated by gauge bosons at a fundamental level [2]. Conventional and high temperature superconductivity is caused by interaction mediated by lattice phonons or spins [3], and effective interactions between bosons mediated by fermions in an atomic gas have been observed [4–6]. The exquisite single particle control of trapped ions combined with the great flexibility of atomic gases makes hybrid atom-ion systems a promising new platform to systematically explore mediated interactions [7]. In such a system, the induced interaction between ions mediated by the surrounding atoms can be controlled using the many experimentally tunable parameters of atomic gases, and accurately detected with high precision ion spectroscopy. Remarkable experimental progress has been reported regarding atom-ion collisions, sympathetic cooling, molecular physics [8–14], Rydberg atom-ion mixtures [15,16], and mobile ions in a Bose-Einstein condensate (BEC) [17–20]. Recently, atom-ion Feshbach resonances were observed, opening up the possibility to tune the interaction strength [21]. Theoretically, the properties of a static ion in a BEC were explored [22], and mobile ions have been predicted to form quasiparticles when they are immersed in a BEC [23–25] or a Fermi gas [26], which are charged analogs of neutral Bose and Fermi polarons [6,27–35].

Here, we investigate the interaction between two ions mediated by a surrounding BEC or Fermi gas. Using a combination of analytical and numerical calculations, we show that such hybrid atom-ion systems can be used to accurately probe mediated interactions with ion phonon spectroscopy, and that they can be tuned to new regimes using the flexibility of atomic gases.

Model.—We consider two static ions separated by $\mathbf{R}$ in a spatially homogenous three-dimensional quantum degenerate gas consisting of identical bosonic or fermionic atoms of mass m and density n at zero temperature, see Fig. 1. The Hamiltonian is

$$\hat{H} = \sum_{\mathbf{k}} \frac{k^2}{2m} \hat{c}_{\mathbf{k}}^{\dagger} \hat{c}_{\mathbf{k}} + \frac{g}{2} \sum_{\mathbf{k},\mathbf{k}',\mathbf{q}} \hat{c}_{\mathbf{k}+\mathbf{q}}^{\dagger} \hat{c}_{\mathbf{k}'-\mathbf{q}}^{\dagger} \hat{c}_{\mathbf{k}'} \hat{c}_{\mathbf{k}}$$
$$+ \sum_{\mathbf{k},\mathbf{q}} V_q \hat{c}_{\mathbf{k}+\mathbf{q}}^{\dagger} \hat{c}_{\mathbf{k}} (1 + e^{-i\mathbf{q}\cdot\mathbf{R}}), \quad (1)$$

where $\hat{c}_{\mathbf{k}}^{\dagger}$ creates an atom with momentum $\mathbf{k}$ and $\hat{c}_{\mathbf{k}}\hat{c}_{\mathbf{k}'}^{\dagger} \mp \hat{c}_{\mathbf{k}'}^{\dagger}\hat{c}_{\mathbf{k}} = \delta_{\mathbf{k},\mathbf{k}'}$ for bosons/fermions as usual. The Fourier transform of the atom-ion interaction is V_q and $\hbar$ and the system volume are set to unity. We define $g = 4\pi a_{BB}/m$ with a_{BB} the atom-atom scattering length and $n^{1/3}a_{BB} \ll 1$, so that interaction effects can be described using Bogoliubov theory for bosons. The atom-atom interaction plays no role for a single-component Fermi gas due to Pauli exclusion.

The electric field from the ions gives rise to a long-range atom-ion interaction $-\alpha_{\mathrm{atom}}/2r^4$ with α_{atom} the atom polarizability [7]. The corresponding characteristic length scale $r_{\mathrm{ion}} = \sqrt{2m\alpha}$ where $\alpha = \alpha_{\mathrm{atom}}/2$ can easily be of the same order of magnitude as the average inter-atom distance, so it is crucial to include the long-range $1/r^4$ tail explicitly in our theory [22]. To include the short-range repulsion due to
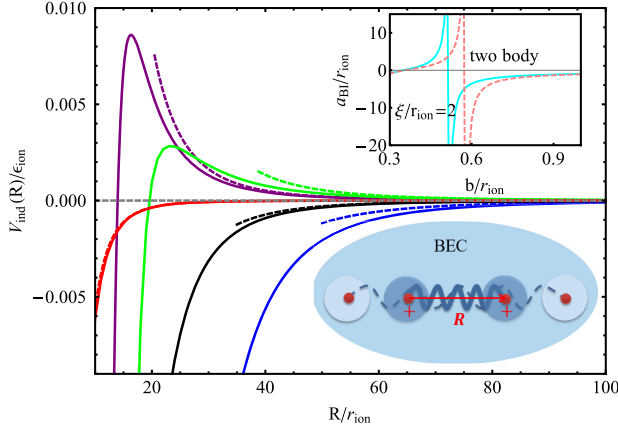
FIG. 1. Illustration: two ions interact via density modulations in the surrounding BEC. This changes the out-of-phase phonon frequency in a linear rf trap. Main plot: the induced interaction $V_{\text{ind}}(R)$ in units of $\epsilon_{\text{ion}} = 1/2mr_{\text{ion}}^2$ between two ions mediated by a BEC with density $nr_{\text{ion}}^3 = 1$, healing length $\xi/r_{\text{ion}} = 2$, and $b/r_{\text{ion}} = 1.4$ (red), 0.53 (black), 0.52 (blue), 0.51 (green), and 0.5 (purple) corresponding to the atom-ion in-medium scattering lengths $r_{\text{ion}}/a_{BI} = -1.641, -0.054, -0.014, 0.029, 0.076$, respectively. The solid lines are the numerical results obtained from Eq. (7), while the dashed lines are the analytical results given by Eqs. (5) and (8). Inset: the atom-ion scattering length a_{BI} in the BEC medium (solid line) and a vacuum $a_{BI,v}$ (dashed line).
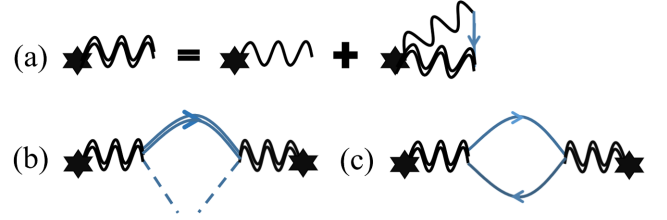

FIG. 2. (a) Diagrams for the atom-ion scattering matrix. A $*$ is an ion, a wavy line is the atom-ion interaction, and a blue line is the atom Green's function. (b) The induced interaction mediated by a sound mode (double line) in a BEC. Dashed lines are condensate atoms. (c) The induced interaction mediated by a particle-hole excitation in a Fermi gas.

the overlap between the atom and ion electron clouds, we use the effective interaction [36]

$$V(r) = -\frac{\alpha}{(r^2 + b^2)^2}\frac{r^2 - c^2}{r^2 + c^2}, \qquad (2)$$

where $b \sim \mathcal{O}(r_{\text{ion}})$ gives the inverse depth of the potential and $c \sim a_0 \ll r_{\text{ion}}$ the transition point between $V(r) > 0$ and $V(r) < 0$. While the full interaction potential is complicated and supports many bound states [7], their energy separation is much larger than the relevant energies for the present many-body problem. It is therefore sufficient to use Eq. (2) with b and c determined so that it recovers the atom-ion scattering length and the energy of the highest bound state of a given atom-ion combination. Here, we fix $c = 0.0023r_{\text{ion}}$ in our numerical calculations and vary b, thereby tuning the strength and presence of the maximally one bound state of Eq. (2). This mimics the tuning of the energy of the highest bound state in a real atom-ion system, which gives rise to the recently observed Feshbach resonances [21].

Atom-ion scattering.—Consider first the scattering of an atom on a static ion. The scattering matrix obeys

$$\mathcal{T}(\mathbf{p}', \mathbf{p}; \omega) = V_{\mathbf{p}'-\mathbf{p}} + \sum_{\mathbf{k}} \mathcal{T}(\mathbf{p}', \mathbf{k}; \omega)G(\mathbf{k}, \omega)V_{\mathbf{k}-\mathbf{p}} \qquad (3)$$

in the ladder approximation, see Fig. 2(a). Here, $\mathbf{p}$ ($\mathbf{p}'$) is the momentum of the incoming (outgoing) atom with

energy ω and $G(\mathbf{k}, \omega)$ is the atom Green's function [37]. Equation (3) is exact in the case of vacuum scattering where $G(\mathbf{k}, \omega) = 1/(\omega - \mathbf{k}^2/2m)$ and the atom-ion scattering length can be obtained as $a_{BI,v} = m\mathcal{T}_{\text{vac}}(0, 0; 0)/2\pi$. When the scattering occurs in the BEC, we use the Bogoliubov Green's function $G(\mathbf{k}, \omega) = u_{\mathbf{k}}^2/(\omega - E_{\mathbf{k}}) - v_{\mathbf{k}}^2/(\omega + E_{\mathbf{k}})$ in Eq. (3), where $E_{\mathbf{k}} = \sqrt{\epsilon_{\mathbf{k}}^2 + 2ng\epsilon_{\mathbf{k}}}$ is the excitation spectrum and $v_{\mathbf{k}}^2 = u_{\mathbf{k}}^2 - 1 = [(\epsilon_{\mathbf{k}} + ng)/E_{\mathbf{k}} - 1]/2$. Then we define the scattering length in the BEC as $a_{BI} = m\mathcal{T}(0, 0; 0)/2\pi$. In the inset of Fig. 1, we plot the scattering length a_{BI} as a function of b in a BEC with healing length $\xi = 1/\sqrt{8\pi na_{BB}} = 2r_{\text{ion}}$. We also plot the scattering length $a_{BI,v}$ in a vacuum for comparison. The scattering diverges at $b \simeq 0.5168r_{\text{ion}}$ where a bound atom-ion state emerges. We see that this is a smaller value of b than for the vacuum case corresponding to a deeper atom-ion interaction potential, which shows that the BEC suppresses the formation of bound states. When the scattering occurs in a Fermi gas, we use the Fermi Green's function $G(\mathbf{k}, \omega) = 1/(\omega - k^2/2m + \epsilon_F)$ with $\epsilon_F = k_F^2/2m = (6\pi^2 n)^{2/3}/2m$ the Fermi energy. Since scattering at the Fermi surface is the most important, we define the scattering length in a Fermi gas as $a_{FI} = m\text{Re}[\mathcal{T}_s(k_F, k_F; 0)]/2\pi$, where the subscript s represents the s-wave component. The scattering matrix has poles at the bound state energies of an atom in the potential of the ion, and $\mathcal{T}(0, 0; 0)$ diverges every time a new bound state appears. We have $\mathcal{T}_{\mathbf{R}}(\mathbf{p}', \mathbf{p}; \omega) = \mathcal{T}(\mathbf{p}', \mathbf{p}; \omega)\exp[-i(\mathbf{p}' - \mathbf{p}) \cdot \mathbf{R}]$ for the scattering matrix of the ion at position $\mathbf{R}$.

BEC and weak interaction.—We now analyze the induced interaction between two ions in a BEC, considering first the case of a weak atom-ion interaction $b \gtrsim r_{\text{ion}}$ so that there is no shallow two-body bound state. The induced interaction can then be extracted rigorously from a perturbative calculation of the energy shift due to the presence of the two ions. To first order, we obtain the Hartree shift $E_1 = 2nV_{q=0}$, which does not depend on their separation $\mathbf{R}$. The second order energy shift is [38]

$$E_2 = \sum_{\mathbf{q}} V_q^2[1 + \cos(\mathbf{q} \cdot \mathbf{R})]\chi(q, 0) = \tilde{E}_2 + V_{\text{ind}}(R) \qquad (4)$$

with $\chi(q,0)$ the static density-density response function of the gas. The constant term $\tilde{E}_2$ is the second order energy shift coming from each ion separately, whereas we can identify the $\mathbf{R}$ dependent part as the induced interaction $V_{\text{ind}}(\mathbf{R})$ between the two ions. Note that Eq. (4) holds for both fermions and bosons.

For a BEC, the static density-density correlation function is $\chi(q,0) = -4nm/(q^2 + 2/\xi^2)$ to leading order in $n^{1/3}a_{BB}$. Using this in Eq. (4), one finds [38]

$$V_{\text{ind}}(R) = \frac{mV_{q=0}}{2\pi a_{BB}}\frac{\alpha}{R^4} \qquad (5)$$

for $R \gg b, c, \xi$. Thus, the long-range induced interaction is proportional to $1/R^4$ like the bare atom-ion interaction with a magnitude given by $\sim (m\alpha^2\pi)/(2a_{BB}r_{\text{ion}}R^4) \sim (mr_{\text{ion}}a_{BB})^{-1}(r_{\text{ion}}/R)^4$ where we have used $V_{q=0} \sim \alpha\pi^2/r_{\text{ion}}$. It is also inversely proportional to the Bose-Bose scattering length a_{BB}, reflecting that a more compressible BEC leads to a stronger induced interaction.

For shorter distance with $b, c \ll R \lesssim \xi$, Eq. (4) can also be evaluated analytically giving [38]

$$V_{\text{ind}}(R) = -\pi^3 nm\alpha^2 \frac{(b^2+c^2)^2}{b^2(b^2-c^2)^2}\frac{1}{R}e^{-\sqrt{2}R/\xi}. \qquad (6)$$

This has the same functional form as the Yukawa interaction obtained for neutral impurities in a BEC [39,40].

BEC and strong interaction.—For strong atom-ion interactions, we must include the atom-ion scattering matrix in the induced interaction between the two ions. The dominant contribution is the exchange of a sound mode in the BEC, see Fig. 2(b). This gives [38]

$$V_{\text{ind}}(R) = \sum_{\mathbf{k}} \mathcal{T}(\mathbf{k},0;0)^2 \chi(\mathbf{k},0)\cos(\mathbf{k}\cdot\mathbf{R}) \qquad (7)$$

where we have used the symmetry $\mathcal{T}(\mathbf{k},\mathbf{k}';\omega) = \mathcal{T}(\mathbf{k}',\mathbf{k};\omega)$. Comparing to Eq. (4), we see that the strong coupling result is obtained by substituting the bare atom-ion interaction by the scattering matrix.

When $R \gg [b, c, \xi, m\mathcal{T}(0,0;0)]$, Eq. (7) gives [38]

$$V_{\text{ind}}(R) = \frac{m\mathcal{T}(0,0;0)}{2\pi a_{BB}}\frac{\alpha}{R^4}. \qquad (8)$$

Hence, the induced interaction is proportional to $1/R^4$ as for the weak interaction case, when R is much larger than the characteristic length scale r_{ion} and the spatial size of the bound state that emerges at resonance. It follows from Eq. (8) that the interaction is very strong close to resonance where a new atom-ion dimer state becomes stable and $\mathcal{T}(0,0;0)$ diverges. In addition, Eq. (8) shows that the sign of $V_{\text{ind}}(R)$ is determined by $\mathcal{T}(0,0;0)$.

In Fig. 1, the induced interaction potential between two ions in a BEC with density $nr_{\text{ion}}^3 = 1$, healing length $\xi/r_{\text{ion}} = 2$, and different values of b (or a_{BI}) is plotted. $V_{\text{ind}}(R)$ increases with increasing depth of the atom-ion interaction potential (decreasing b), except close to the nodes, becoming very large as the resonance value $b \simeq 0.5168r_{\text{ion}}$ is approached and a bound atom-ion state emerges. Interestingly, $V_{\text{ind}}(R)$ has a node when $b/r_{\text{ion}} < 0.5168$ so that it is repulsive in the long-range limit, since $\mathcal{T}(0,0;0)$ changes sign when a bound state enters the potential, see Eq. (8). Figure 1 clearly shows how the strength and sign of the induced interaction depend critically on the shape of the atom-ion interaction and the presence of a bound state.

Fermi gas and weak interaction.—We now turn to the case of two ions in a single component Fermi gas exploring first weak atom-ion interactions so that Eq. (4) is valid. The density-density correlation function of a Fermi gas is $\chi(q,0) = \sum_{\mathbf{k}}(f_{\mathbf{k}} - f_{\mathbf{k}+\mathbf{q}})/(\xi_{\mathbf{k}} - \xi_{\mathbf{k}+\mathbf{q}})$ [41], where $f_{\mathbf{k}} = [\exp(\beta\xi_{\mathbf{k}}) + 1]^{-1}$ is the Fermi function and $\xi_{\mathbf{k}} = k^2/2m - \epsilon_F$. Using this in Eq. (4), we can derive [38]

$$V_{\text{ind}}(R) = \begin{cases} \frac{mk_F}{\pi^2}V_{q=0}\frac{\alpha}{R^4} & b \gg k_F^{-1} \\ \gamma\frac{2k_F R\cos(2k_F R)-\sin(2k_F R)}{R^4} & b, c \ll k_F^{-1} \end{cases} \qquad (9)$$

with $\gamma = \pi m\alpha^2(b^2+c^2)^2/16b^2(b^2-c^2)^2$ for $R \gg b, c$. Note that the second line is of the Ruderman-Kittel-Kasuya-Yosida form, which is the same as the mediated interaction between two impurities in a Fermi gas where the impurity-fermion interaction is short range [42–44]. This shows that the atom-ion interaction can be treated as short range when the typical interparticle spacing is larger than r_{ion}. In the high density regime on the other hand, the interaction has the same $1/R^4$ form as for a BEC, Eq. (5), although its strength is reduced by $2k_F a_{BB}/\pi \ll 1$ reflecting that the Fermi gas is much less compressible than the BEC.

Fermi gas and strong interaction.—For strong atom-ion interaction, we again include the scattering matrix in the induced interaction. The exchange of particle-hole excitations in the Fermi gas between the ions give [38]

$$V_{\text{ind}}(R) = \sum_{\mathbf{q},\mathbf{k}}\left[2\theta(k_F - k)\frac{\text{Re}[\mathcal{T}^2(\mathbf{k}+\mathbf{q},\mathbf{k};\xi_{\mathbf{k}})]}{\xi_{\mathbf{k}} - \xi_{\mathbf{k}+\mathbf{q}}}\right.$$
$$\left. - \int_{-\epsilon_F}^{0}\frac{d\omega}{\pi}\frac{\text{Im}[\mathcal{T}^2(\mathbf{k}+\mathbf{q},\mathbf{k};\omega+i\eta)]}{(\omega-\xi_{\mathbf{k}+\mathbf{q}})(\omega-\xi_{\mathbf{k}})}\right]\cos(\mathbf{q}\cdot\mathbf{R}),$$
$$(10)$$

see Fig. 2(c). We have assumed zero temperature and zero population of any bound states.

In Fig. 3, the induced interaction given by Eq. (10) is plotted for the density $k_F r_{\text{ion}} = 0.1$ and various values of b.
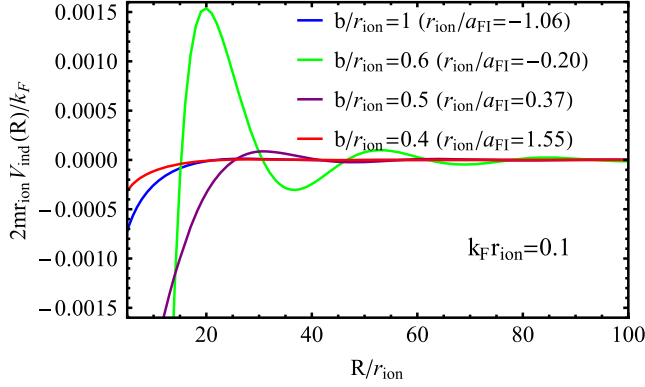
FIG. 3. Induced interaction between two ions in a Fermi gas with the density $k_F r_{ion} = 0.1$ and different values of b (or a_{FI}) controlling the strength of the atom-ion interaction.

Only the s-wave channel of the atom-ion scattering contributes for this low density, which simplifies the numerics significantly. Figure 3 shows that the interaction increases with decreasing b towards $b = 0.575 r_{ion}$ where a bound state appears at the Fermi surface. Friedel oscillations characteristic of an interaction mediated by a Fermi sea are clearly visible. As the bound state energy decreases with decreasing $b < 0.575 r_{ion}$, the interaction again decreases reflecting that it becomes off-resonant.

Experimental probing.—We now show that the induced interaction leads to shifts in the phonon spectrum of trapped ions. Consider two ions in a linear rf trap with trapping frequencies $\omega_y, \omega_z \gg \omega_x$. The slow dynamics in the assumed rf-field free x direction is determined by [45]

$$U = \frac{\kappa}{2}(x_2^2 + x_1^2) + \frac{Z^2 e^2}{4\pi\epsilon_0}\frac{1}{x_2 - x_1} + V_{ind}(x_2 - x_1), \quad (11)$$

where x_j is the x coordinate of ion j with $x_2 > x_1$ and Ze is the ion charge. The first term is the electrostatic trapping potential with a force constant κ, the second is the Coulomb interaction, and the third the mediated interaction between the two ions. Even though the equilibrium distance between the ions is affected by the induced interaction [38], it is typically difficult to measure without dramatically perturbing the ion-atom system.

A more promising approach is to measure the phonon spectrum of the ions with high accuracy through a single blue sideband excitation to a long-lived electronic state by a narrow bandwidth laser, followed by detecting fluorescence addressing a different fast decaying transition [46]. The frequency $\omega_x = \sqrt{\kappa/M}$ of the Kohn mode where the two ions oscillate in-phase is independent of any interaction between the ions. Note that the effective mass M can be different from the bare ion mass due to the dressing by the surrounding BEC [24,25]. This effect is distinct from those due to the induced interaction, and it can be determined by measuring the oscillation frequency ω_x of a *single* ion—a
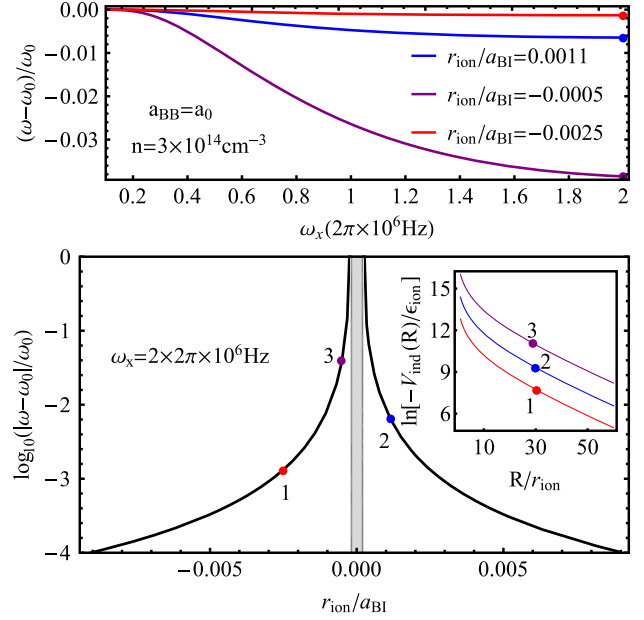

FIG. 4. The relative frequency shift of the out-of-phase mode due to the induced interaction as a function of the trap frequency ω_x (top), and as a function of the ^{7}Li-^{138}Ba$^+$ scattering length a_{BI} (bottom). The inset shows the induced interaction for the three scattering lengths in the upper panel. The dots show the frequency shifts and equilibrium distances (inset) for the three scattering lengths and $\omega_x = 4\pi \times 10^6$ Hz.

procedure that has been used for a neutral impurity in a Fermi gas [47].

Contrary to the Kohn mode, the mode where the two ions oscillate out-of-phase (see the illustration of Fig. 1) is affected by the induced interaction. In the top panel of Fig. 4, we plot its frequency obtained from Eq. (11) by evaluating the relevant second derivatives of the induced interaction around the equilibrium positions numerically, compared to its value $\omega_0 = \sqrt{3}\omega_x$ in the absence of the induced interaction. We use parameters m, $M = m_{ion}$, and α appropriate for a ^{7}Li-^{138}Ba$^+$ mixture. The BEC density is $n = 3 \times 10^{14}$ cm^{-3}, which gives $nr_{ion}^3 = 0.136$ when $r_{ion} = 76.8$ nm. Also, $\xi/r_{ion} = 20.6$ corresponding to $a_{BB} = a_0$. This is an approximate value for the ^{7}Li-^{7}Li scattering length in a wide range of magnetic fields [48,49], where one expects several ^{7}Li-^{138}Ba$^+$ Feshbach resonances based on recent experimental results [21]. The frequency shift in Fig. 4 increases with trapping frequency reflecting the increased strength of the induced interaction compared to the Coulomb repulsion for shorter distances. It is negative for all scattering lengths because the equilibrium distance R_0 between the ions is so short that the induced interaction is attractive as seen explicitly in the inset of Fig. 4. When $R_0 \gg a_{BI} > 0$ and Eq. (8) holds, the induced interaction is positive leading to a positive frequency shift [38]. Since we are close to resonance, this however requires a very large trap size. A positive frequency shift for reasonable values of

R_0 can be obtained with a smaller a_{BI} away from resonance, but it will be small and difficult to be observed. The shift has the largest magnitude close to $r_{\mathrm{ion}}/a_{BI} = 0$ where a new atom-ion bound state appears. In the Supplemental Material, we show frequency shifts for the case of a $^{87}\mathrm{Rb}$-$^{87}\mathrm{Rb}^+$ (or $^{87}\mathrm{Sr}^+$) mixture [38].

The bottom panel of Fig. 4 shows the frequency shift as a function of the atom-ion scattering length a_{BI} in the BEC using the same parameters as in the upper panel of Fig. 4 and a trapping frequency $\omega_x = 4\pi \times 10^6$ Hz. Since a realistic experimental resolution is $\Delta\omega/\omega \gtrsim 10^{-4}$, the figure shows that the mediated interaction is observable for $|a_{BI}| \gtrsim 100 r_{\mathrm{ion}} \sim 1.5 \times 10^5 a_0$. The accuracy in magnetic field tuning required to achieve such a large value depends on the width of the specific ion-atom Feshbach resonance at hand, but assuming widths of 10–100G and typical field fluctuations of a few mG, this should be realistic to achieve. Indeed, scattering lengths of the same order of magnitude were realized in neutral atomic gases more than a decade ago [48]. Close to resonance where a bound state emerges and $1/a_{BI} = 0$, the induced interaction exceeds the Coulomb repulsion leading to an instability as indicated by the gray region in the lower panel of Fig. 4. Because the induced interaction in a Fermi gas is weaker than in a BEC due to its smaller compressibility, it will be harder to observe and may require larger trapping frequencies.

Conclusions and outlook.—We analyzed the interaction between two ions mediated by a BEC or a Fermi gas. For weak atom-ion interactions, we derived several analytical results, and our theory was then generalized to strong atom-ion interactions. Finally, we discussed how the control and precision of hybrid ion-atom systems can be used to probe these mediated interactions systematically and in new regimes.

Our results motivate future work in several directions. It would be interesting to explore the effects of populating the bound states, which may give rise to an additional attractive interaction [50]. Since the micromotion energy of the ions is of the same order of magnitude as the critical temperature of the BEC $T_c \sim \mathcal{O}(\mu\mathrm{K})$, a key question concerns temperature and heating effects. We expect our results to be accurate when the condensate fraction $1 - (T/T_c)^3$ is close to unity. It is also important to explore the three-body recombination rate [51,52], which in addition to loss also may lead to heating and molecule population. Using a Fermi gas may be advantageous for reducing such processes. Other fascinating problems include the induced interaction in a strongly correlated Fermi gas in the BEC-BCS crossover, and between two mobile ions. Finally, it would be useful to apply approaches such as Monte Carlo calculations to the challenging strongly interacting regime [53].

[*]bruungmb@phys.au.dk

[1] G. Baym and C. Pethick, *Landau Fermi-Liquid Theory: Concepts and Applications* (Wiley-VCH, New York, 1991).

[2] S. Weinberg, *The Quantum Theory of Fields* (Cambridge University Press, Cambridge, England, 1995), Vol. 1.

[3] D. Scalapino, Phys. Rep. **250**, 329 (1995).

[4] B. J. DeSalvo, K. Patel, G. Cai, and C. Chin, Nature (London) **568**, 61 (2019).

[5] H. Edri, B. Raz, N. Matzliah, N. Davidson, and R. Ozeri, Phys. Rev. Lett. **124**, 163401 (2020).

[6] I. Fritsche, C. Baroni, E. Dobler, E. Kirilov, B. Huang, R. Grimm, G. M. Bruun, and P. Massignan, Phys. Rev. A **103**, 053314 (2021).

[7] M. Tomza, K. Jachymski, R. Gerritsma, A. Negretti, T. Calarco, Z. Idziaszek, and P. S. Julienne, Rev. Mod. Phys. **91**, 035001 (2019).

[8] A. T. Grier, M. Cetina, F. Oručević, and V. Vuletić, Phys. Rev. Lett. **102**, 223201 (2009).

[9] C. Zipkes, S. Palzer, C. Sias, and M. Köhl, Nature (London) **464**, 388 (2010).

[10] A. Härter, A. Krükow, A. Brunner, W. Schnitzler, S. Schmid, and J. H. Denschlag, Phys. Rev. Lett. **109**, 123201 (2012).

[11] L. Ratschbacher, C. Zipkes, C. Sias, and M. Köhl, Nat. Phys. **8**, 649 (2012).

[12] T. Sikorsky, Z. Meir, R. Ben-Shlomi, N. Akerman, and R. Ozeri, Nat. Commun. **9**, 920 (2018).

[13] T. Feldker, H. Fürst, H. Hirzler, N. Ewald, M. Mazzanti, D. Wiater, M. Tomza, and R. Gerritsma, Nat. Phys. **16**, 413 (2020).

[14] J. Schmidt, P. Weckesser, F. Thielemann, T. Schaetz, and L. Karpa, Phys. Rev. Lett. **124**, 053402 (2020).

[15] T. Secker, R. Gerritsma, A. W. Glaetzle, and A. Negretti, Phys. Rev. A **94**, 013420 (2016).

[16] T. Secker, N. Ewald, J. Joger, H. Fürst, T. Feldker, and R. Gerritsma, Phys. Rev. Lett. **118**, 263201 (2017).

[17] K. S. Kleinbach, F. Engel, T. Dieterle, R. Löw, T. Pfau, and F. Meinert, Phys. Rev. Lett. **120**, 193401 (2018).

[18] T. Dieterle, M. Berngruber, C. Hölzl, R. Löw, K. Jachymski, T. Pfau, and F. Meinert, Phys. Rev. A **102**, 041301(R) (2020).

[19] T. Dieterle, M. Berngruber, C. Hölzl, R. Löw, K. Jachymski, T. Pfau, and F. Meinert, Phys. Rev. Lett. **126**, 033401 (2021).

[20] C. Veit, N. Zuber, O. A. Herrera-Sancho, V. S. V. Anasuri, T. Schmid, F. Meinert, R. Löw, and T. Pfau, Phys. Rev. X **11**, 011036 (2021).

[21] P. Weckesser, F. Thielemann, D. Wiater, A. Wojciechowska, L. Karpa, K. Jachymski, M. Tomza, T. Walker, and T. Schaetz, Nature (London) **600**, 429 (2021).

[22] P. Massignan, C. J. Pethick, and H. Smith, Phys. Rev. A **71,** 023606 (2005).

[23] W. Casteels, J. Tempere, and J. Devreese, J. Low Temp. Phys. **162,** 266 (2011).

[24] G. E. Astrakharchik, L. A. P. Ardila, R. Schmidt, K. Jachymski, and A. Negretti, Commun. Phys. **4,** 94 (2021).

[25] E. R. Christensen, A. Camacho-Guardian, and G. M. Bruun, Phys. Rev. Lett. **126,** 243001 (2021).

[26] E. R. Christensen, A. Camacho-Guardian, and G. M. Bruun, Phys. Rev. A **105,** 023309 (2021).

[27] N. B. Jørgensen, L. Wacker, K. T. Skalmstang, M. M. Parish, J. Levinsen, R. S. Christensen, G. M. Bruun, and J. J. Arlt, Phys. Rev. Lett. **117,** 055302(R) (2016).

[28] M.-G. Hu, M. J. Van de Graaff, D. Kedar, J. P. Corson, E. A. Cornell, and D. S. Jin, Phys. Rev. Lett. **117,** 055301 (2016).

[29] L. A. Peña Ardila, N. B. Jørgensen, T. Pohl, S. Giorgini, G. M. Bruun, and J. J. Arlt, Phys. Rev. A **99,** 063607 (2019).

[30] Z. Z. Yan, Y. Ni, C. Robens, and M. W. Zwierlein, Science **368,** 190 (2020).

[31] A. Schirotzek, C.-H. Wu, A. Sommer, and M. W. Zwierlein, Phys. Rev. Lett. **102,** 230402 (2009).

[32] C. Kohstall, M. Zaccanti, M. Jag, A. Trenkwalder, P. Massignan, G. M. Bruun, F. Schreck, and R. Grimm, Nature (London) **485,** 615 (2012).

[33] M. Koschorreck, D. Pertot, E. Vogt, B. Fröhlich, M. Feld, and M. Köhl, Nature (London) **485,** 619 (2012).

[34] P. Massignan, M. Zaccanti, and G. M. Bruun, Rep. Prog. Phys. **77,** 034401 (2014).

[35] F. Scazza, G. Valtolina, P. Massignan, A. Recati, A. Amico, A. Burchianti, C. Fort, M. Inguscio, M. Zaccanti, and G. Roati, Phys. Rev. Lett. **118,** 083602 (2017).

[36] M. Krych and Z. Idziaszek, Phys. Rev. A **91,** 023430 (2015).

[37] H. Bruus and K. Flensberg, *Many-Body Quantum Theory in Condensed Matter Physics: An Introduction* (Oxford University Press, Oxford, 2004).

[38] See Supplemental Material at http://link.aps.org/supplemental/10.1103/PhysRevLett.129.153401 includes the derivation of the formula to calculate induced interaction and its analytical expression at large distance. It also presents the results of the equilibrium distance between two ions and the relative frequency shift of the out-of-phase phonon mode in a linear rf trap for ^{7}Li-^{138}Ba$^+$ mixture and ^{87}Rb-^{87}Rb$^+$ (or ^{87}Sr$^+$) mixture. The analytical frequency shift when Eq. 8 holds is also discussed.

[39] A. Camacho-Guardian and G. M. Bruun, Phys. Rev. X **8,** 031042 (2018).

[40] A. Camacho-Guardian, L. A. Peña Ardila, T. Pohl, and G. M. Bruun, Phys. Rev. Lett. **121,** 013401 (2018).

[41] J. Lindhard, Kgl. Dan. Vid. Selsk. Mat.-Fys. Medd. **28,** 8 (1954).

[42] M. A. Ruderman and C. Kittel, Phys. Rev. **96,** 99 (1954).

[43] T. Kasuya, Prog. Theor. Phys. **16,** 45 (1956).

[44] K. Yosida, Phys. Rev. **106,** 893 (1957).

[45] D. James, Appl. Phys. B **66,** 181 (1998).

[46] G. Poulsen, Ph.D. thesis, Aarhus University, 2011.

[47] S. Nascimbène, N. Navon, K. J. Jiang, L. Tarruell, M. Teichmann, J. McKeever, F. Chevy, and C. Salomon, Phys. Rev. Lett. **103,** 170402 (2009).

[48] S. E. Pollack, D. Dries, M. Junker, Y. P. Chen, T. A. Corcovilos, and R. G. Hulet, Phys. Rev. Lett. **102,** 090402 (2009).

[49] P. S. Julienne and J. M. Hutson, Phys. Rev. A **89,** 052715 (2014).

[50] T. Enss, B. Tran, M. Rautenberg, M. Gerken, E. Lippi, M. Drescher, B. Zhu, M. Weidemüller, and M. Salmhofer, Phys. Rev. A **102,** 063321 (2020).

[51] B.-B. Wang, Y.-C. Han, W. Gao, and S.-L. Cong, Phys. Chem. Chem. Phys. **19,** 22926 (2017).

[52] B.-B. Wang, S.-H. Jing, and T.-X. Zeng, J. Chem. Phys. **150,** 094301 (2019).

[53] L. A. Peña Ardila and A. Negretti (private communications).